AAS 19-267

EXPLORING THE LOW-THRUST TRAJECTORY DESIGN SPACE FOR SMALLSAT MISSIONS TO THE SUN-EARTH TRIANGULAR EQUILIBRIUM POINTS

Christopher J. Sullivan,[*] Ian Elliott,[*] Natasha Bosanac,[†] Farah Alibay,[‡] and Jeffrey R. Stuart[§]

With the increasing availability of upcoming rideshare opportunities, low-thrust-enabled small satellites could be leveraged as a platform for targeted heliophysics investigations conducted from the Sun-Earth L4 or L5 regions. In the early stages of mission concept development for small satellites, understanding the trajectory trade space and the influence of the spacecraft hardware configuration and scientific objectives is crucial. Fundamental dynamical structures within the Sun-Earth system are examined and used to extract insight into the properties of the trajectory design space for low-thrust-enabled small satellites to visit Sun-Earth L4 or L5 from several fixed deployment conditions.

INTRODUCTION

Using dynamical systems theory as the basis for developing low-thrust trajectory design methods enables the exploration of solar processes via low-thrust-enabled small satellites (SmallSats). For instance, the Sun-Earth L4 and L5 points are of interest to the heliophysics community due to their nominally stable orbit properties and their locations: approximately 60° ahead of and trailing the Earth in its heliocentric orbit, respectively. Placing an observational platform at either point would enable the scientific community to observe numerous heliophysics processes, including coronal mass ejections (CMEs) and solar energetic particles (SEPs), from a vantage point that does not lie on the Sun-Earth line.[1] Additionally, placing spacecraft at either equilibrium point supports the development of an early warning system for solar storms, potentially reducing damage to both space and Earth-based assets.[2] While both points have previously been visited by the Solar TErrestial RElations Observatory A/B (STEREO-A/B) spacecraft, neither of these spacecraft entered into an orbit about L4 or L5.[3,4] Furthermore, the utility of follow-on heliophysics-based science missions to Sun-Earth L4 and L5 has been consistently identified and resulted in a number of proposals with varying objectives and architectures.[1,2,5–10] However, leveraging dynamical systems theory to explore the trajectory design space for low-thrust-enabled SmallSats may potentially enable similar heliophysics-based science objectives to be accomplished at an even lower cost. With numerous

[*]Graduate Research Assistant, Smead Department of Aerospace Engineering Sciences, University of Colorado Boulder, Boulder CO, 80309.

[†]Assistant Professor, Colorado Center for Astrodynamics Research, Smead Department of Aerospace Engineering Sciences, University of Colorado Boulder, Boulder CO, 80309.

[‡]Systems Engineer, Jet Propulsion Laboratory, California Institute of Technology, Pasadena CA, 91109.

[§]Mission Design and Navigation Systems Engineer, Jet Propulsion Laboratory, California Institute of Technology, Pasadena CA, 91109.

rideshare opportunities anticipated in the coming decade, there is potential for a low-cost SmallSat mission to visit either of these Lagrange points from a fixed deployment condition to perform heliophysics-based scientific observation. Future rideshare opportunities may include a number of cislunar missions such as Exploration Mission-1 (EM-1) or a follow-in mission, as well as missions designed to place a space telescope near Sun-Earth L1 or L2.

While SmallSats may provide a viable low-cost option for achieving a targeted science return, they introduce significant challenges into the trajectory design process. Trajectory designers must contend with the additional challenges that the SmallSat form factor imposes including: low maneuverability due to a limited propulsive capability, constrained deployment conditions, and operational scheduling constraints due to limited power. These challenges all impact the availability and geometry of feasible transfer paths that tend to exist in a high-dimensional design space.[11] Efficiently exploring this space to analyze the wide array of flight times and required propellant masses requires a guided approach to trajectory design.

Insights from dynamical systems techniques have been demonstrated to be valuable for recovering a point design in the complex solution space associated with SmallSat trajectories in multi-body gravitational environments.[11,12] Using fundamental dynamical structures, such as periodic orbits and invariant manifolds – that sufficiently predict the flow structures in higher-fidelity gravitational models – as well as information from zero-velocity surfaces and Poincaré mapping strategies enables construction of an informed trajectory design process. Bosanac, Cox, Howell and Folta demonstrate this approach for Lunar IceCube, a low-thrust-enabled CubeSat that leverages multi-body dynamics to operate in the lunar vicinity.[11] In addition, Bosanac, Alibay, and Stuart demonstrated that a dynamical systems approach, with inputs based on the hardware and operational concept, supports identification of a feasible trajectory for a CubeSat deployed from a previous iteration of an EM-1 deployment condition to reach and orbit about L5.[12] Building upon this contribution, Elliott, Sullivan, Bosanac, Alibay, and Stuart improve upon this method to rapidly design trajectories to the Sun-Earth triangular equilibrium points from a fixed deployment condition, demonstrated in the context of spacecraft with two form factors: a SmallSat and a 6U CubeSat.[13] In this method, the authors use a combination of high-fidelity dynamical models and approximations via the Circular Restricted Three-Body Problem (CR3BP). This approach accurately captures the motion of the spacecraft within cislunar space during the sensitive post-deployment phase, while reducing the complexity of analysis during phases where the CR3BP offers a sufficient prediction of fundamental flow structures. Using these models in combination, natural and low-thrust arcs are rapidly and efficiently assembled into a discontinuous initial guess that is transitioned to an ephemeris model. To recover smooth, continuous trajectories that inherit the properties of the initial guess, a multiple shooting corrections scheme is then applied.

This analysis leverages the approach demonstrated by Elliott, Sullivan, Bosanac, Alibay, and Stuart for a preliminary exploration of the solution space of feasible trajectories for low-thrust-enabled SmallSats to reach the triangular equilibrium points, while incorporating the significant hardware and operational constraints of SmallSats.[12] For this analysis, the spacecraft form factor is held constant. Then, two fundamental parameters are considered as input variables to the preliminary design space exploration: the deployment condition and the target equilibrium point (i.e., L4 or L5). First, three near-Earth deployment conditions are examined. Recovery of end-to-end trajectories for each these distinctly different deployment conditions provides heuristics for mission concept development and a preliminary overview of constraints on feasible rideshare opportunities. Then, for each deployment scenario, the target equilibrium is varied. Identifying feasible point designs for a Small-

Sat to reach both L4 and L5 during mission concept development supports exploration of potential mission architectures (i.e., single or dual launches) and planning of science objectives. The recovery of feasible solutions for each of these driving variables indicate the potential for SmallSats to reach the Sun-Earth triangular equilibrium points to perform low-cost, targeted science.

DESIGN SPACE DEFINITION

For this analysis, the form factor of the spacecraft is held constant. Specifically, an ESPA-class SmallSat equipped with a Hall-effect thruster, modeled with a constant thrust and constant I_{sp}, is considered representative of near-term technology.[12,14] The high-level characteristics of this SmallSat are displayed in Table 1, consistent with the analysis performed by Bosanac, Alibay, and Stuart.[12] Analysis of these design parameters reveals that only a low level of thrust is available to the SmallSat. Thus, long, continuous thrust arcs, while also leveraging the underlying dynamics in the chaotic gravitational environment, may be required for significant adjustments to the path of the spacecraft. Given the high I_{sp} associated with this propulsion system, year-long finite burns can be leveraged along the trajectory without a large depletion of the available propellant mass. However, the limited power capabilities inherent to the SmallSat form factor restricts the number of other operational tasks, i.e. for science, navigation and communication, that can be accomplished during these burns. In subsequent analyses, short coast arcs would need to be included approximately every week to dedicate power to these tasks. In the meantime, however, it is assumed that the end-to-end trajectory would generally retain the geometry of the preliminary designs in this analysis following incorporation of these regular coast arcs. Finally, any feasible trajectory must deliver the SmallSat to its final science orbit with enough time to complete its scientific objectives prior to reaching its maximum lifetime. Most CubeSat missions have been in the LEO environment and no definitive deep-space lifetime has yet been demonstrated. Accordingly, we prioritize reduced times-of-flight within our design process to mitigate uncertainty in component lifetime.

Table 1. Assumed SmallSat characteristics

Parameter	ESPA SmallSat[12]
Initial Wet Mass (kg)	180
Maximum Propellant Mass (kg)	40
Available Thrust (mN)	13
I_{sp} (s)	1375
Available Propellant Power (W)	200

To begin the preliminary design space exploration, a number of design parameters were identified that significantly influence the geometry of available solutions. For instance, Figure 1 displays the SmallSat form factor in black that was considered fixed throughout this investigation, the deployment condition in blue that was varied, and the target region in red that was also modified to explore the design space centered on this class of trajectories. Since an ESPA-class SmallSat could potentially leverage a variety of rideshare opportunities, the deployment condition is considered an input variable in a preliminary design space exploration. In this analysis, three deployment conditions are considered to both demonstrate the robustness of a dynamical systems approach and to explore the differences in the feasibility and geometry of low-thrust trajectories for SmallSats. These three deployment scenarios are designed to be representative of rideshare opportunities in the following three types of missions: (1) a cislunar mission, (2) a space telescope to a northern Sun-Earth L1 quasi-halo orbit, and (3) a space telescope bound for a southern Sun-Earth L2 quasi-halo orbit.

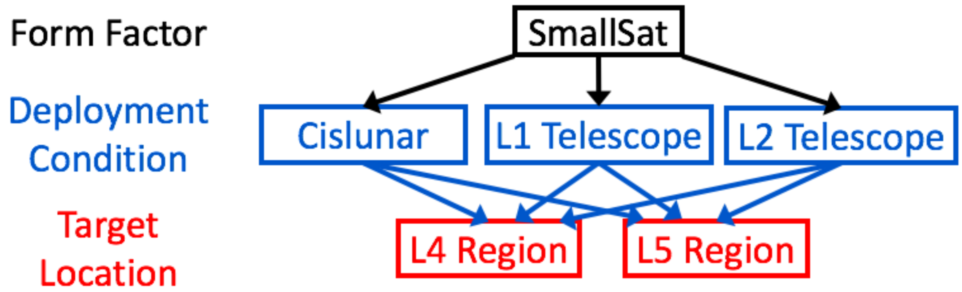

Figure 1. Defining the fixed design parameters in black, the input design parameters in blue, and the output parameters in red for exploring the design space of low-thrust SmallSat trajectories to a triangular equilibrium point in the Sun-Earth system.

An additional input variable in this design space exploration is the target equilibrium point since Sun-Earth L4 and L5 both serve as suitable vantage points for space-based, heliophysics research.[1] For instance, both points offer a three-dimensional perspective on solar phenomenon outside of the existing observatories stationed along the Sun-Earth line. Furthermore, the stability of orbits in the vicinity of either point indicates the need for relatively minimal station keeping maneuvers. In addition, two spacecraft each positioned at one of the triangular equilibrium points would enable multi-point measurements. However, due to the Sun's rotation, locating a spacecraft at L5 does offer some distinct advantages over L4 by providing a 4-5 day early warning system for CMEs prior to Earth impact, thereby serving to protect assets including satellites, observatories, and astronauts.[5,12]

DYNAMICAL MODELS

Models of various levels of fidelity are leveraged to develop an initial guess for a trajectory prior to corrections in a point mass ephemeris model. One useful dynamical model is the CR3BP which admits natural dynamical structures that are used to rapidly construct a trajectory, guide the design process, and more efficiently explore the design space.[15] In addition to utilizing these dynamical structures, low-thrust segments within a low-thrust-enabled CR3BP model are implemented to adjust the solution, connecting arcs at distinctly different energy levels and opening otherwise inaccessible regions of the system. Using these two dynamical models, an initial guess is assembled. To transition these trajectories to a high-fidelity ephemeris model, a multiple-shooting corrections scheme is employed. This procedure is summarized briefly here; additional details are discussed by Elliott, Sullivan, Bosanac, Alibay and Stuart.[13]

Circular Restricted Three-Body Problem

The CR3BP is an autonomous model that can be efficiently explored via dynamical systems techniques.[15] This model reflects the motion of a small body of negligible mass under the gravitational influence of two larger primaries with mass M_i, each assumed to follow circular orbits about their mutual barycenter.[16] In addition, a rotating frame, denoted $\hat{x}\hat{y}\hat{z}$ and displayed in Figure 2, is defined using the two primaries. In this frame, the $\hat{x}$ axis is directed from the larger primary to the smaller primary, the $\hat{z}$ axis is in the direction of the angular momentum of the system, and the $\hat{y}$ axis completes the right-handed coordinate system. Furthermore, position, time, and mass parameters are typically nondimensionalized using the system's characteristic quantities, denoted l^*, t^*, and m^*. First, l^* is defined as the distance between the two primaries, t^* is selected to set the mean motion

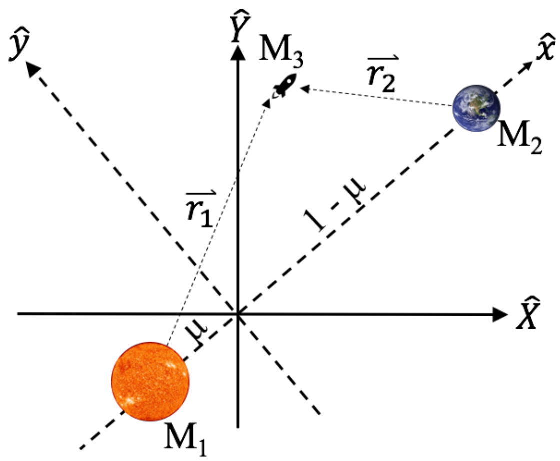

Figure 2. Definition of the Sun-Earth rotating frame, $\hat{x}\hat{y}\hat{z}$, relative to the inertial frame, $\hat{X}\hat{Y}\hat{Z}$.

of the primaries to unity, and m^* is defined as the sum of the masses of the two primaries. Then, the mass ratio of the system is defined as $\mu = \frac{M_2}{m^*}$; the value of this quantity influences the availability and geometry of the dynamical structures. Using these definitions, the state of the spacecraft is written as $\vec{x} = [x, y, z, \dot{x}, \dot{y}, \dot{z}]$, capturing the nondimensionalized position and velocity of the spacecraft in the rotating frame and relative to the system's barycenter. Then, the nondimensional equations of motion for the natural motion of a spacecraft are written as:

$$\ddot{x} - 2\dot{y} = \frac{\partial U^*}{\partial x} \quad \ddot{y} + 2\dot{x} = \frac{\partial U^*}{\partial y} \quad \ddot{z} = \frac{\partial U^*}{\partial z} \tag{1}$$

where $U^* = \frac{1}{2}(x^2+y^2)+\frac{1-\mu}{r_1}+\frac{\mu}{r_2}$ is the pseudo-potential function while $r_1 = \sqrt{(x+\mu)^2 + y^2 + z^2}$ and $r_2 = \sqrt{(x-1+\mu)^2 + y^2 + z^2}$. These equations of motion in the CR3BP admit an integral of motion labeled the Jacobi constant, equal to $C_J = 2U^* - \dot{x}^2 - \dot{y}^2 - \dot{z}^2$. This parameter is an energy-type quantity that determines the accessible regions of the system, providing valuable insight into constructing an itinerary and heuristics for designing maneuvers. As an example, consider two periodic orbits that are described by distinct values of the Jacobi constant. To design a transfer between these orbits in the CR3BP, energy must either be added or removed via low-thrust or impulsive maneuvers.

A variety of natural dynamical structures exist in the CR3BP including equilibrium points, periodic orbits, quasi-periodic orbits, and invariant manifolds.[17] The equilibrium, or Lagrange points, are commonly denoted as L_1, L_2, and L_3 for the collinear points and L_4 and L_5 for the triangular points. For a mass ratio corresponding to the Sun-Earth system, L_1, L_2, and L_3 possess stable and unstable modes indicating that motion naturally approaches or departs these equilibrium points as well as oscillatory modes corresponding to the existence of periodic orbits. These periodic orbits exist in continuous families; members of these families that are unstable possess stable and unstable manifolds that also guide natural motion towards and away from the associated periodic orbits.[17] These manifolds offer a natural transport mechanism within the system, including towards the L_4 and L_5 points. Similarly, L_4 and L_5 possess only oscillatory modes at this mass ratio indicating the existence of periodic orbits emanating from each point. Periodic orbits about the L_4 and L_5 equilibrium points in the Sun-Earth system tend to possess nominally stable geometries. With no stable or unstable invariant manifolds, an additional acceleration is required in order to insert into these orbits. One method of inserting into these orbits is by using a low-thrust engine to gradually adjust the path of the spacecraft and guide motion into these stable orbits.

Low-Thrust-Enabled CR3BP

To identify arcs for insertion into stable periodic orbits about the L_4 and L_5 points, the acceleration associated with a constant thrust and constant I_{sp} engine is added to the equations of motion of the CR3BP. First, a nondimensionalized acceleration, $\vec{a}$, imparted on the spacecraft is calculated as:

$$\vec{a} = \frac{T_{nd}}{m_{s/c,nd}}\hat{u} = a_x\hat{x} + a_y\hat{y} + a_z\hat{z} = a_v\hat{v} + a_n\hat{n} + a_c\hat{c} \tag{2}$$

where T_{nd} denotes the nondimensional thrust, $m_{s/c,nd}$ captures the current nondimensionalized spacecraft mass at the time of the maneuver, and $\hat{u}$ is a unit vector reflecting the thrust direction. This unit vector is convenient to express for a velocity-normal-conormal (VNC) frame defined with respect to the Earth: $\hat{V}$, $\hat{N}$, $\hat{C}$ correspond to the velocity, normal, and conormal directions respectively. This VNC frame is used due to its operational advantages during mission planning and execution.[11] However, when expressed in the VNC frame, the acceleration must undergo a coordinate transformation to the rotating frame to accurately model the resulting acceleration on the spacecraft in the CR3BP.[18] After this transformation, the equations of motion that capture a low-thrust perturbation to the CR3BP are written as:

$$\ddot{x} - 2\dot{y} = \frac{\partial U^*}{\partial x} + a_x \quad \ddot{y} + 2\dot{x} = \frac{\partial U^*}{\partial y} + a_y \quad \ddot{z} = \frac{\partial U^*}{\partial z} + a_z \tag{3}$$

Since the acceleration depends on the spacecraft mass, the state is redefined to capture the spacecraft mass, i.e., $\vec{x}_{LT} = [x, y, z, \dot{x}, \dot{y}, \dot{z}, m_{s/c}]$. To model the decrement in the spacecraft mass due to propellant mass usage, an additional first-order equation augments the equations of motion. This equation is written as $\dot{m}_{s/c} = \frac{-T}{I_{sp}g_0}$, where g_0 is the gravitational acceleration on the surface of Earth, $9.81 m/s^2$.[19]

Low-Thrust-Enabled Point Mass Ephemeris Model

Following construction of an initial guess in the CR3BP, the guess must be transitioned to a point mass ephemeris model. In this higher-fidelity model, the motion of the primaries is no longer assumed to be perfectly circular about their mutual barycenter and gravity due to additional bodies is captured. In the point mass ephemeris model, the state vector of the spacecraft is written as $\vec{X} = [X, Y, Z, \dot{X}, \dot{Y}, \dot{Z}, m_{s/c}]$ with position and velocity components nondimensionalized via the characteristic quantities of the Sun-Earth system and defined in an Earth-centered inertial frame.[11,20] The nondimensional equations of motion for this model are then written in vector form:

$$\ddot{\vec{R}}_{E,s/c} = -GM_E\left(\frac{\vec{R}_{E,s/c}}{R^3_{E,s/c}}\right) + GM_i\left(\frac{\vec{R}_{s/c,i}}{R^3_{s/c,i}} - \frac{\vec{R}_{E,i}}{R^3_{E,i}}\right) + \vec{a}_{ECI} \tag{4}$$

where $\vec{R}_{E,s/c} = [X, Y, Z]$ represents the position vector of the spacecraft from Earth, $\vec{R}_{s/c,i}$ defines the nondimensionalized position vector locating body i with respect to the spacecraft, M_i designates the nondimensionalized mass of body i, G denotes the nondimensionalized standard gravitational parameter, and $\vec{a}_{ECI}$ is the normalized acceleration due to the thrust, transformed from the VNC frame to the Earth-centered inertial frame. Similarly, a first-order equation governing the change in the mass of the spacecraft due to the application of thrust is written as $\dot{m}_{s/c} = \frac{-T}{I_{sp}g_0}$. The ephemeris model is inherently nonautonomous: any trajectory is dependent on the epoch. Furthermore, the equations of motion require knowledge of the location of each celestial body relative to the spacecraft. To incorporate this ephemeris data for the Earth, Sun, and Moon, the DE421 data file is accessed via NASA's SPICE toolkit.[21,22] Additional bodies and perturbations, namely J2 and solar radiation pressure (SRP), could be included in a higher-fidelity model, however these additional gravitational bodies tend to most significantly influence the trajectory of the spacecraft for this itinerary.

CORRECTIONS SCHEME

Once an initial guess for a trajectory is constructed using arcs that exist in the CR3BP, a multiple shooting corrections scheme is employed to recover a nearly continuous solution in a low-thrust-enabled point mass ephemeris model.[20] First, the initial guess is discretized into a sequence of arcs described by the position, velocity, spacecraft mass, and epoch at the beginning of each arc as well as the associated integration time. For arcs generated in the CR3BP, the initial position and velocity vectors must be transformed from the rotating frame to an inertial frame. Propagating the nodes at the beginning of each arc forward in time in the point mass ephemeris model leads to discontinuities between neighboring arcs. These discontinuities are the result of the additional gravitational influence of the Moon and the primaries no longer following a circular orbit. To correct the discontinuities and identify a nearby continuous solution, a multiple shooting corrections scheme is employed. In this formulation of a multiple shooting scheme, Newton's method is used to iteratively and simultaneously update the variables describing every arc until a continuous solution is recovered. Satisfaction of the continuity constraints ensures continuity in position, velocity, mass, and time agreement along the entire solution. This approach reduces the sensitivity of the corrections, enables incorporation of additional constraints, and supports connecting natural and low-thrust arcs. As a result, an end-to-end solution that possesses a similar geometry to the initial guess is recovered.

DESIGN SPACE EXPLORATION: ITINERARY CONSTRUCTION

To construct an initial guess, the general itinerary of an end-to-end trajectory is defined. Each segment along this trajectory is analyzed using insights from dynamical systems theory to informatively select coast and low-thrust segments. While Elliott, Sullivan, Bosanac, Alibay and Stuart provide a detailed overview of this process, this section outlines useful insights specific to understanding the impact of the deployment condition and target equilibrium point on the existence and geometry of feasible solutions.[13]

Natural Transport Mechanisms in the Sun-Earth System

To gain preliminary insight into the influence of the deployment condition on the design space, dynamical systems theory is used to analyze the associated natural path. In particular, a path that begins near the Earth vicinity must pass through either the Sun-Earth L1 or L2 gateway to travel towards either of the Sun-Earth triangular equilibrium points. These gateways are visualized using the intersection of zero velocity surfaces with the xy-plane; labeled zero velocity curves. An example of zero velocity curves constructed at a Jacobi constant between that of L2 and L4 is illustrated in Figure 3 in the Sun-Earth rotating frame in dimensional coordinates. Gray shading corresponds to forbidden regions while white indicates allowable regions of motion. Overlaid on this figure are

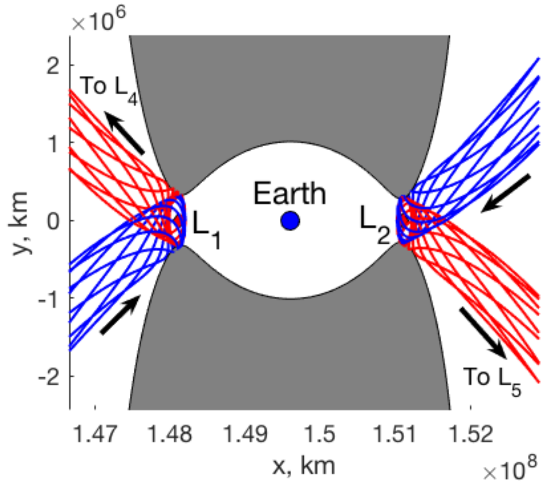

Figure 3. Using stable (blue) and unstable (red) manifolds associated with L1 and L2 Lyapunov orbits to visualize natural transport mechanisms in the Sun-Earth CR3BP, with zero velocity curves displayed in gray.

the stable (blue) and unstable (red) manifolds associated with L1 and L2 Lyapunov orbits. These manifolds tend to govern the flow towards and away from the gateways. Using Figure 3 as a reference, these manifolds offer valuable insight for itinerary construction. Specifically, motion that naturally approaches the vicinity of L5 must pass through the L2 gateway, while paths that approach L4 originate from the L1 gateway.[17] As the value of the Jacobi constant is decreased – or the energy is increased – these gateways open even further. Decreasing the Jacobi constant further towards the value corresponding to L4 or L5, the intersections of the zero velocity surfaces with the xy plane collapse to the equilibrium points. At lower values of the Jacobi constant, these zero velocity surfaces exist solely out of the plane. These observations suggest that, for a spacecraft to reach L5 from a near-Earth deployment condition with a value of the Jacobi constant between that of L2 and L5, the spacecraft energy must be increased; this change in energy is achieved via a low-thrust maneuver. Furthermore, if the natural trajectory associated with a deployment condition initially tends towards L1, low-thrust maneuvers may be used to alter the path to pass through the L2 gateway and approach L5.

Natural Motions After Deployment

Each of the three deployment conditions considered in this analysis is propagated in the point mass ephemeris model to reveal the associated natural motion within the Earth vicinity. These natural trajectories are visualized in the Sun-Earth rotating frame to facilitate the use of dynamical systems theory and comparison to natural transport mechanisms in the CR3BP.

Cislunar Deployment: This deployment condition corresponds to a previous iteration of a high-energy, near-Earth, cislunar-type state at an epoch of October 21, 2024. Propagating this deployment condition forward in time for 180 days in the point mass ephemeris model of the Sun, Earth and Moon produces the natural trajectory depicted in Figure 4. In this figure, a blue arc represents the natural trajectory in the Sun-Earth rotating frame in dimensional coordinates. The Moon's path is plotted in gray and the Sun-Earth L1 and L2 equilibrium points are located by red diamonds. Analysis of this trajectory reveals that a lunar flyby occurs - yet, the spacecraft would not pass through either the L1 or L2 gateways in a reasonable time. This observations suggests that low-

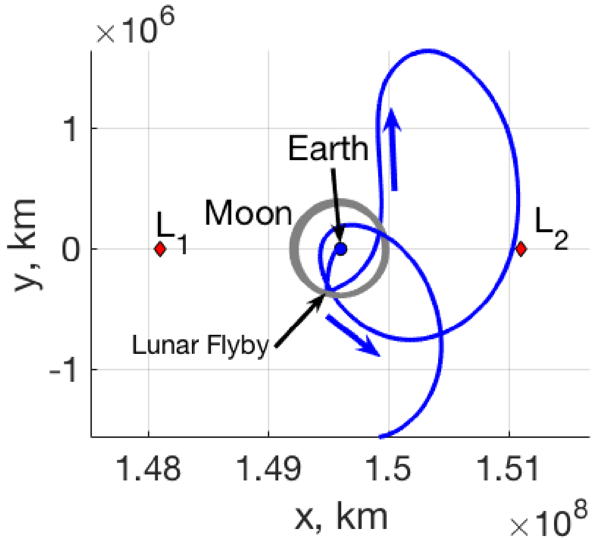

Figure 4. Natural path (blue) associated with a previous iteration of the cislunar deployment condition in the Sun-Earth rotating frame.

thrust maneuvers and/or an adjustment of the lunar flyby conditions are necessary for the trajectory to pass through one of these two gateways.

Deployment from an L1 Space Telescope Mission: Consider a SmallSat serving as a secondary payload on a mission for a space telescope destined for a northern quasi-halo orbit near Sun-Earth L1. It is assumed that the SmallSat would be deployed approximately 24 hours after departure from low Earth orbit on January 2, 2025. Naturally propagating this initial state forward in time in a point mass ephemeris model produces the trajectory plotted in Figure 5, using a configuration and color scheme consistent with Figure 4. This natural trajectory does possess the necessary energy to depart

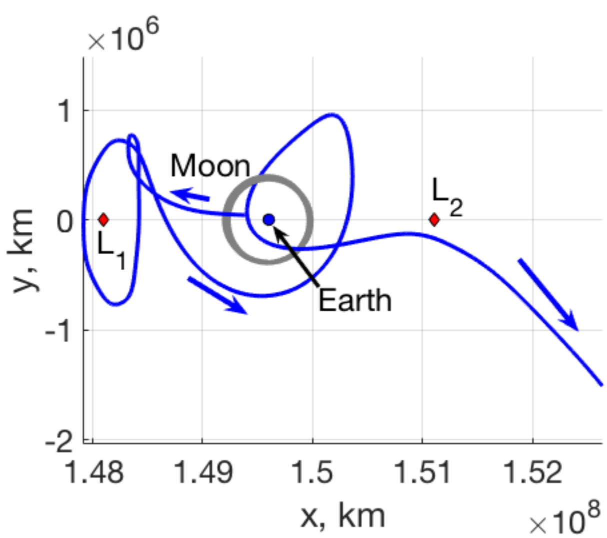

Figure 5. Natural path (blue) associated with deployment from a space telescope destined for Sun-Earth L1, depicted in the rotating frame.

the Earth vicinity through one of the gateways. First, the spacecraft completes one revolution of the Sun-Earth L1 point prior to performing a single revolution around the Earth and then departing through the L2 gateway. While this deployment condition does eventually pass through the L2 gateway, strategically placed burns could be leveraged to potentially eliminate the revolution around the Earth and the reduce the time to depart through the L2 gateway.

Deployment from an L2 Space Telescope Mission: If, however, the space telescope is destined for a southern quasi-halo orbit in the Sun-Earth L2 region, a distinctly different deployment condition is defined. Retaining the same initial epoch of January 2, 2025, and integrating a sample initial state vector forward in time in a point mass ephemeris model produces the natural trajectory plotted in Figure 6, using a color scheme and configuration consistent with Figure 4.This particular trajectory passes directly through the Sun-Earth L2 gateway in a short time interval. Accordingly, the spacecraft does possess the necessary energy to escape through the gateways without additional flybys or burns – although low-thrust maneuvers may be used for small path adjustments. To guide the spacecraft to escape through the L1 gateway, however, low-thrust maneuvers are certainly required.

Candidate Science Orbits

Periodic orbits in the CR3BP offer an initial prediction of bounded motions in the vicinity of Sun-Earth L4 or L5. Fundamental orbit families that emanate from these triangular equilibrium points include, the planar short period, planar long period and three-dimensional vertical orbits. Since the natural motion of the spacecraft following any of the three deployment conditions examined in this analysis exhibits only a small deviation out of the plane of the primaries, candidate orbits for the science phase of a trajectory are limited to the planar short and long period families near L4 and L5. Due to their simple geometry, consider the short period families: selected members along this family, close to the equilibrium points, are plotted in dimensional coordinates in the Sun-Earth rotating frame in Figures 7(a) and 7(b). In these figures, the Sun and Earth are located by filled circles while the equilibrium points are indicated with red diamonds and arrows indicate direction of motion. As these orbits evolve away from L4 or L5, they grow in size and the Jacobi

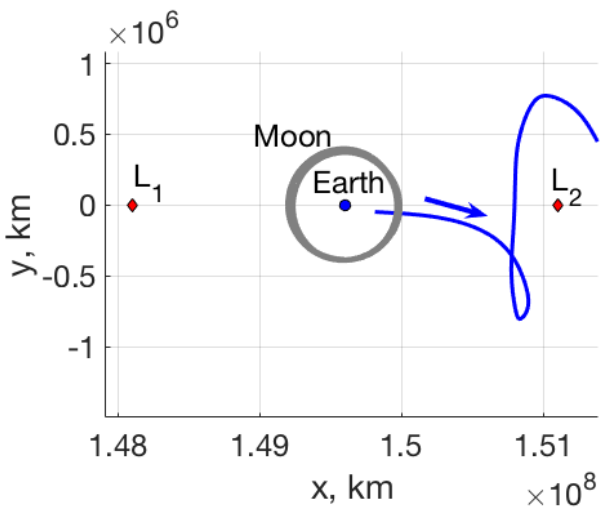

Figure 6. Natural path (blue) associated with deployment from a space telescope destined for Sun-Earth L2, depicted in the rotating frame.

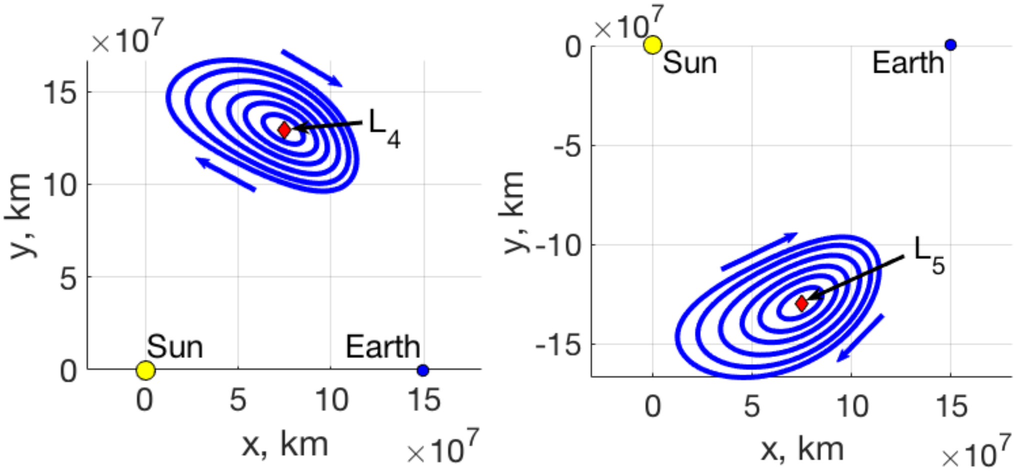

(a) (b)

Figure 7. Selected members of the L4 and L5 short period orbit families in the Sun-Earth system in Figures 7(a) and 7(b) respectively.

constant decreases. One orbit in the plotted portion of each family is selected for initial guess construction, each possessing a Jacobi constant of 2.995 in the Sun-Earth rotating frame. Of course, subsequent analyses may consider the impact of the selected science orbit on the properties of the initial guess. Nevertheless, each of the two selected science orbits – one around L4 and one around L5 – is stable.[16] Accordingly, a low-thrust maneuver is required to enter the orbit. To design this insertion burn, a thrust time of one year is selected to provide sufficient time to both increase the spacecraft's energy and significantly adjust its path, while using less than the available propellant mass. Using the approach outlined by Elliott, Sullivan, Bosanac, Alibay and Stuart, several insertion burns are generated by integrating backwards in time from the science orbit with the low-thrust engine activated.[13] Poincaré mapping is then used to identify feasible arcs for incorporation into the initial guess.

DESIGN SPACE EXPLORATION: PRELIMINARY RESULTS

Using the general itineraries outlined in the previous section, continuous solutions are developed for a SmallSat with the hardware parameters listed in Table 1. The approach used to construct each trajectory is outlined in Elliott, Sullivan, Bosanac, Alibay and Stuart.[13] In this preliminary exploration of the design space, a single point design is constructed for each combination of the three deployment conditions and two target science orbits. The characteristics of each end-to-end trajectory are analyzed and compared.

Accessing the L5 Region from Various Deployment Conditions

Deployment from an L2 Space Telescope Mission: First, a trajectory for a SmallSat travelling to the Sun-Earth L5 region from a deployment condition representative of a rideshare opportunity on a Sun-Earth L2 telescope mission is presented. For this scenario, an end-to-end trajectory is recovered; this solution is displayed in Figure 8(a). This figure depicts the trajectory from deployment to the science phase in the Sun-Earth rotating frame using dimensional coordinates. Coast segments are colored blue and the low-thrust arcs are displayed in red. Additionally, the Sun-Earth

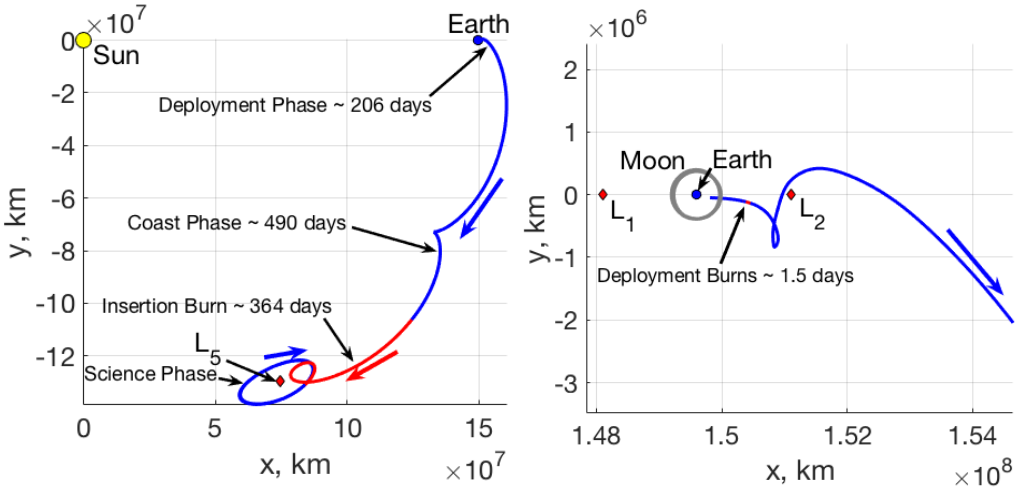

(a) (b)

Figure 8. Planar projection of a low-thrust trajectory delivering a SmallSat to the Sun-Earth L5 region, leveraging a rideshare opportunity on a space telescope mission to Sun-Earth L2: (a) complete transfer and (b) zoomed-in view of the Earth vicinity. Coast arcs are displayed in blue and low-thrust segments in red.

L5 point appears near the center of the bounded science orbit via a red diamond. Using the zoomed-in view in Figure 8(b) as a reference, the trajectory leverages a 1.5 day low-thrust maneuver in the $0.40\hat{v} - 0.77\hat{n} + 0.48\hat{c}$ direction after deployment and once the spacecraft has left the Earth-Moon system. The spacecraft then passes through the Sun-Earth L2 gateway and travels towards the L5 region naturally. During this phase of the trajectory secondary scientific measurements could be performed between regular navigation and communication activities. After approximately 490 days of natural motion, a 364 day low-thrust maneuver is applied in approximately the $0.36\hat{v}+0.77\hat{n}+0.53\hat{c}$ direction. Then, the spacecraft inserts into a short period orbit near L5. This trajectory requires only 30.4278 kg of propellant, below the available propellant mass of 40 kg. Furthermore, the transfer requires 2.9 years from deployment to the end of insertion burn. Once in the nominal science orbit, scientific observation, communication, navigation, and other operations may be performed for the remainder of the spacecraft lifetime.

Deployment from an L1 Space Telescope Mission: A continuous solution is constructed for the SmallSat to visit Sun-Earth L5 following deployment from a telescope bound for the Sun-Earth L1 region. The resulting trajectory is displayed in Figure 9(a) with a configuration and coloring consistent with Figure 8(a); a zoomed-in view of the Earth vicinity appears in Figure 9(b). This particular trajectory requires that the spacecraft perform two low-thrust maneuvers with a combined length of 1.06 days in the Earth vicinity. The spacecraft then follows a natural path resembling a Sun-Earth L2 halo manifold with a low time of flight, suitable inclination, and links to a science orbit insertion arc. The first maneuver is directed along the velocity vector and the second maneuver is in the $-0.80\hat{v} - 0.31\hat{n} - 0.51\hat{c}$ direction. Recall that the natural motion following deployment for this scenario eventually departed through the L2 gateway - however, the natural path exhibited a single revolution in the vicinity of L1. Since halo orbits near L1 tend to possess an orbit period of approximately 180 days, removal of this extra revolution via a low-thrust maneuver reduces the time for the spacecraft to pass through the L2 gateway. Accordingly, the end-to-end trajectory in Figure

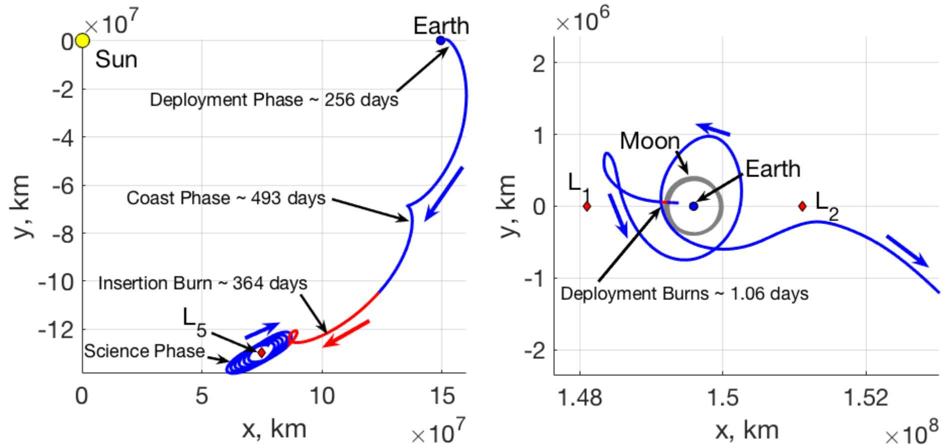

(a) (b)

Figure 9. Planar projection of a low-thrust trajectory delivering a SmallSat to the Sun-Earth L5 region, leveraging a rideshare opportunity on a space telescope mission to Sun-Earth L1: (a) complete transfer and (b) zoomed-in view of the Earth vicinity. Coast arcs are displayed in blue and low-thrust segments in red.

9(a) requires only a slightly longer flight time of 3.09 years in comparison to the previous example. This slight increase in the flight time is attributed to the additional time spent in the Earth vicinity prior to escaping through the L2 gateway. Furthermore, after the 1.06 day deployment maneuvers, the spacecraft travels naturally from the vicinity of L1 to the L2 gateway. This transfer within the Earth vicinity resembles a heteroclinic connection between two periodic orbits about the Sun-Earth L1 and L2 equilibrium points, indicating the value of incorporating natural transport mechanisms within the Earth vicinity in subsequent analyses.[17] In addition, due to the construction of the initial guess and the incorporation of a year long maneuver in the $0.39\hat{v}+0.77\hat{n}+0.50\hat{c}$ direction to insert into an L5 science orbit, this trajectory requires a similar propellant mass to the previous case. Of course, each revolution along the final science orbit displayed in Figure 9(a) are not as tightly bound to one another as in the previous solution. However, the spacecraft does remain bound to the vicinity of L5 for several years. Furthermore, the multiple shooting algorithm leveraged in this analysis does not explicitly constrain the characteristics of the final science orbit. Additional modifications to the low-thrust insertion burn to this point design may be employed to recover a nearby solution with alternative characteristics near L5. Nevertheless, this end-to-end trajectory reveals that efficiently placing burns within the highly sensitive region near the Earth can enable a SmallSat to access L5 from this deployment scenario.

Cislunar Deployment: A point solution is constructed for the SmallSat to reach L5 from a cislunar deployment condition. This trajectory, pictured in Figure 10(a) with a configuration and color scheme consistent with Figure 8(a), follows a similar geometry to the previous two trajectories with the exception of post-deployment segments within the Earth-Moon system and prior to departure through the Sun-Earth L2 gateway. A zoomed-in view of this region is displayed in Figure 10(b). Following a brief 6 hour low-thrust maneuver in the $-0.80\hat{v} - 0.31\hat{n} - 0.51\hat{c}$ direction, a lunar flyby occurs with an altitude of 1,020 km. With this flyby, the spacecraft possesses the necessary energy to escape through the L2 gateway. To demonstrate this observation, the Jacobi constant is evaluated along the trajectory during the post-deployment phase and plotted in red in Figure 11.

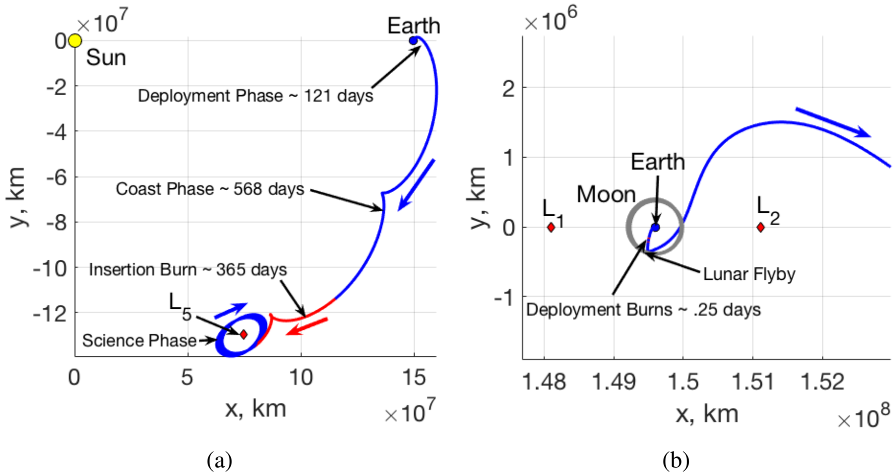

Figure 10. Planar projection of a low-thrust trajectory delivering a SmallSat to the Sun-Earth L5 region, leveraging a rideshare opportunity: (a) complete transfer and (b) zoomed-in view of the Earth vicinity. Coast arcs are displayed in blue and low-thrust segments in red.

Of course, this quantity is evaluated along a solution that is generated in a point mass ephemeris model. Accordingly, it is not expected to remain constant along natural arcs. Nevertheless, this quantity can still provide fundamental insight into naturally accessibly regions of motion. Overlaid on this plot, in blue, is the Jacobi constant evaluated along the naturally propagated trajectory, previously displayed in Figure 4. The values of the Jacobi constant at Sun-Earth L2 and L5 are also depicted in dashed lines. Using Figure 11 as a reference, the low-thrust-enabled trajectory possesses a significantly lower Jacobi constant, closer to that of L5, as it passes through the L2 gateway. In addition, the total flight time from deployment to science orbit insertion for the continuous solution in Figure 8(a) is equal to 2.90 years with a required propellant mass of 30.4279 kg. The majority of this propellant is used to implement the year-long insertion burn in the $0.38\hat{v} + 0.78\hat{n} + 0.51\hat{c}$ direction. However, careful placement of a brief finite burn prior to the flyby enables construction of a trajectory that quickly leaves through the L2 gateway and reaches the vicinity of L5.

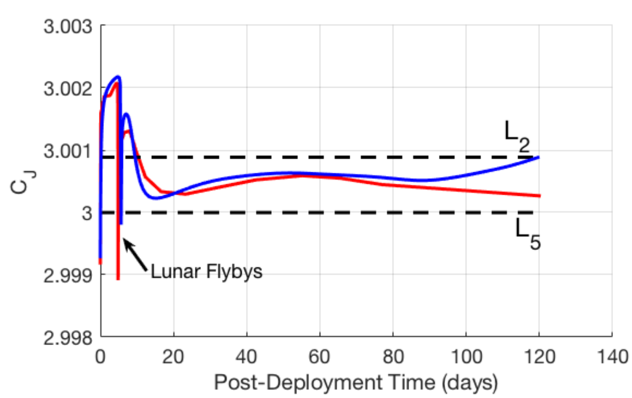

Figure 11. Jacobi constant, in red, along the end-to-end solution between a cislunar deployment condition and L5, displayed for the post-deployment phase. The blue curve indicates the value along the natural post-deployment transfer.

The three computed end-to-end trajectories demonstrate the ability to use a dynamical systems approach to design solutions for a SmallSat to reach L5 from a variety of representative rideshare opportunities. Table 2 summarizes the characteristics of each of these trajectories. The increased flight time for the trajectory associated with a deployment from a telescope bound for Sun-Earth L1 may be attributed to the additional time spent in the Earth vicinity prior to escaping through the L2 gateway. However, additional low-thrust segments may be leveraged to reduce the number of revolutions of the spacecraft around the Earth in future analyses. Nevertheless, the similarity in required propellant mass across the solutions is driven by the initial guess for the L2 to L5 insertion segment, and may not correspond to the minimum values. This initial exploration of the design space for low-thrust SmallSat trajectories to L5 from each of these three deployment conditions suggests that a variety of high-energy near-Earth deployment conditions may be accommodated. In addition, the flight times and required propellant masses in Table 2 offer a useful heuristic during mission concept development.

Accessing the L4 Region from Various Deployment Conditions

To support the design of a mission concept requiring simultaneous deployment of two SmallSats to L4 and L5, an initial exploration of the solution space for low-thrust trajectories to L4 is necessary. Construction of a trajectory that approaches an L4 science orbit follows a similar procedure to the previous cases - however, with the exception that the trajectories must escape through the L1 gateway. Solutions are presented for each of the three deployment conditions and their characteristics are compared.

Deployment from an L2 Space Telescope Mission: For this deployment condition, corresponding to a rideshare opportunity on a telescope bound for Sun-Earth L2, an end-to-end trajectory is displayed in Figure 12(a) with a configuration and color scheme consistent with Figure 8(a). In addition, Figure 12(b) depicts a zoomed-in view near the Earth vicinity. Recall that the natural trajectory associated with this deployment condition quickly passes through the L2 gateway. Adding a brief low-thrust maneuver does adjust the trajectory enough to travel through the Earth vicinity and pass through the L1 gateway. However, including only a small maneuver would require the spacecraft to complete a revolution around the Earth. Thus, for this solution, a longer low-thrust maneuver of approximately 50 days in the $0.72\hat{v} + 0.69\hat{n} - 0.01\hat{c}$ direction is added. This burn sufficiently alters the trajectory to quickly reach the vicinity of L1. After direct passage through the L1 gateway, the spacecraft follows a natural coasting segment that resembles an arc along an L1 halo manifold. Then, a shorter low-thrust maneuver of 315 days in the $0.99\hat{v} + 0.07\hat{c}$ direction is employed for insertion into a tightly bound orbit near L4. This shorter insertion burn, along with a long low-thrust-enabled arc near the Earth, produces a trajectory with a flight time of 2.57 years; shorter than previous solutions. This solution requires a propellant mass of only 30.4242 kg. Although this quantity is already below the maximum available propellant mass, subsequent analyses with optimization or further exploration of the relationship between total maneuver time and flight time may reduce this mass even further.

Table 2. Summary of the characteristics of trajectories to L5 from each of the deployment conditions.

Deployment Condition	Flight time (years)	Required Propellant Mass (kg)
L2 Telescope	2.90	30.4278
L1 Telescope	3.05	30.4287
Cislunar	2.90	30.4279

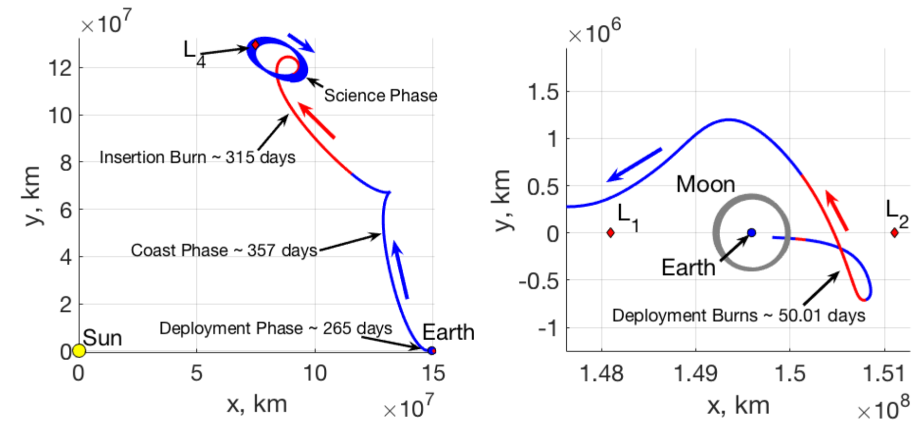

(a) (b)

Figure 12. Planar projection of a low-thrust trajectory delivering a SmallSat to the Sun-Earth L4 region, leveraging a rideshare opportunity on a space telescope mission to Sun-Earth L2: (a) complete transfer and (b) zoomed-in view of the Earth vicinity. Coast arcs are displayed in blue and low-thrust segments in red.

Deployment from an L1 Space Telescope Mission: For the deployment condition associated with a rideshare opportunity on a Sun-Earth L1 bound telescope, a trajectory is recovered that rapidly departs the Earth vicinity. This end-to-end solution is displayed in Figure 13(a) with a configuration and color scheme consistent with Figure 8(a). Figure 13(b) displays a zoomed-in view of the Earth vicinity. For this point design, a brief low-thrust maneuver is applied beyond the radius of the Moon's orbit. This maneuver occurs over approximately 0.68 days in the $0.35\hat{v} - 0.70\hat{n} - 0.62\hat{c}$ direction. This brief maneuver sufficiently adjusts the trajectory to pass directly

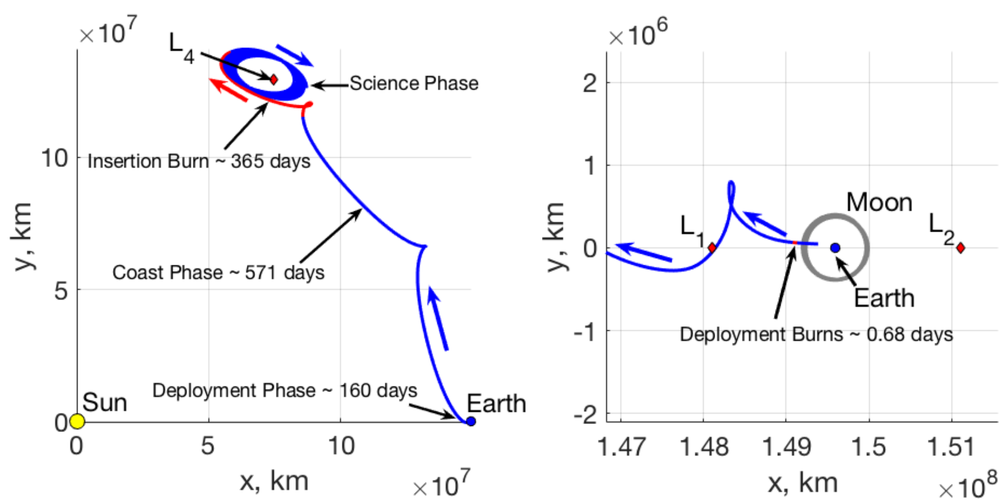

(a) (b)

Figure 13. Planar projection of a low-thrust trajectory delivering a SmallSat to the Sun-Earth L4 region, leveraging a rideshare opportunity on a space telescope mission to Sun-Earth L1: (a) complete transfer and (b) zoomed-in view of the Earth vicinity. Coast arcs are displayed in blue and low-thrust segments in red.

through the L1 gateway. Then, after a long coast segment, a one year low-thrust-enabled insertion is employed with a direction of $0.10\hat{v} - 0.94\hat{n} + 0.32\hat{c}$. Following insertion, the spacecraft exhibits bounded motion in the vicinity of L4. To reach the desired science orbit, the flight time is 3.00 years with a required propellant mass of 30.4261 kg. Compared to the solution for deployment from a Sun-Earth L2 bound telescope rideshare opportunity, this trajectory corresponds to 153 fewer days in the Earth vicinity but more time spent coasting towards L4. Comparison between these two solutions also suggests that further analysis into the complex relationship between the thrust profile and total flight time is warranted.

Cislunar Deployment: An end-to-end trajectory is constructed to connect the cislunar deployment condition to a science orbit near L4, by informatively placing brief maneuvers prior to the lunar flyby. This solution is depicted in Figure 14(a) with a configuration and color scheme consistent with Figure 8(a). A zoomed-in view of the trajectory within the Earth vicinity is displayed in Figure 14(b). This solution leverages a 0.31 day low-thrust maneuver shortly after deployment, aligned with the $0.61\hat{v} - 0.70\hat{n} - 0.37\hat{c}$ direction. Then, a lunar flyby occurs with an altitude of 2,474 km, which is considered operationally feasible. The spacecraft completes less than a revolution around the Earth and quickly passes through the L1 gateway. After a long coast phase, a one year insertion burn occurs with a thrust vector in the $-0.34\hat{v} - 0.76\hat{n} + 0.55\hat{c}$ direction. Several revolutions of a feasible science orbit in the vicinity of L4 are then performed. This end-to-end solution possess a flight time of 3.12 years and requires a propellant mass of 30.4226 kg.

Comparing the three low-thrust trajectories to L4, constructed for each of the three deployment conditions, reveals interesting insights into the complexity of the solution space. Table 3 details the characteristics of each of these trajectories. While the required propellant mass is similar for each trajectory, the flight time varies by up to half a year. The primary reason for this difference in flight time between three trajectories is the placement and duration of the low-thrust maneuvers used to escape the Earth vicinity through the L1 gateway. In fact, for these deployment conditions and a target equilibrium point of L4, these maneuvers varied significantly. These differences suggest

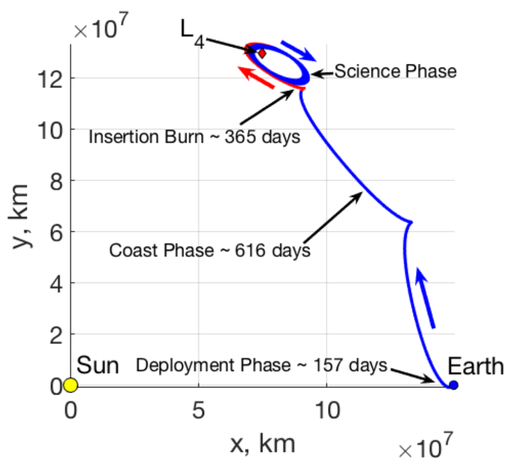

(a)

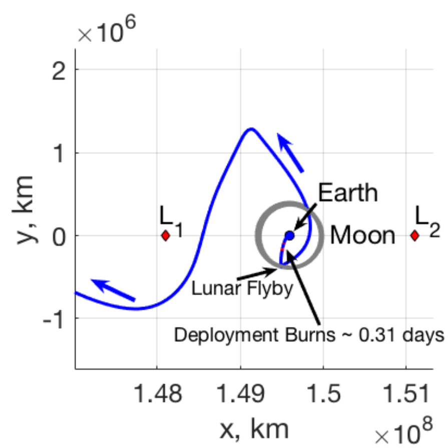

(b)

Figure 14. Planar projection of a low-thrust trajectory delivering a SmallSat to the Sun-Earth L4 region, leveraging a cislunar rideshare opportunity: (a) complete transfer and (b) zoomed-in view of the Earth vicinity. Coast arcs are displayed in blue and low-thrust segments in red.

that the solution space is complex – and additional point designs may reveal a wider variety of flight times and propellant masses for feasible solution. Furthermore, similar differences in the maneuvers may be used to reduce the flight time for the trajectories constructed from each of the deployment conditions to L5. For instance, a longer maneuver may be employed to remove the full revolution around the Earth for the trajectory that reaches L5 from a rideshare opportunity with a space telescope destined for the L1 region, as depicted in Figure 9(a). Nevertheless, the quantities in Table 3 reveal that, through a dynamical systems approach, trajectories to L4 exist for a variety of deployment conditions.

Table 3. Summary of the characteristics of trajectories to L4 from each of the deployment conditions.

Deployment Condition	Flight time (years)	Required Propellant Mass (kg)
L2 Telescope	2.57	30.4243
L1 Telescope	3.00	30.4261
Cislunar	3.12	30.4226

Mission Design Considerations

In addition to demonstrating the value of incorporating dynamical systems techniques into the trajectory design process, the solutions presented in this analysis offer valuable insight for mission concept development. First, end-to-end trajectories exist between each of the deployment conditions and each target equilibrium point, requiring less flight time and propellant mass than the prescribed upper bounds for SmallSat technology. These trajectories indicate the robustness of SmallSat mission concepts that require insertion into an L4 or L5 science orbit to specific rideshare opportunities. Furthermore, the existence of solutions that reach either L4 or L5 from the same deployment condition indicates the significant sensitivity of a trajectory to the thrust profile. Figures 15(a)-15(c) depict zoomed-in views of the Earth vicinity for each of the deployment conditions, with two trajectories – one reaching L4 and one terminating near L5 – overlaid on the same figure. In these figures, red arcs reflect low-thrust burn segments, blue arcs depict coast segments for transfers through the

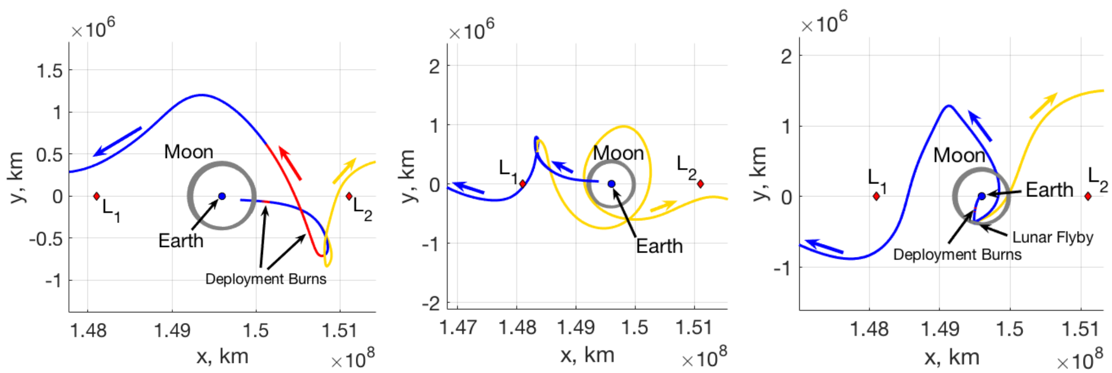

(a) (b) (c)

Figure 15. Overlaid post-deployment phases for trajectories to both L4 and L5 for each of the three deployment conditions: (a) from a telescope traveling to L2, (b) a telescope traveling to L1 and (c) cislunar. Low-thrust arcs are colored red, while coast segments are indicated in blue for the trajectory towards L4 and gold for the trajectory to L5.

L1 gateway, and gold indicates coast arcs for trajectories passing through the L2 gateway. Following the application of low-thrust maneuvers and, in one case, a lunar flyby, these trajectories deviate quickly. This sensitivity may be valuable for recovering from small perturbations to the nominal deployment conditions, or to enable dual launch missions: one SmallSat may be deployed to L4 and another to L5 to perform simultaneous observations from two distinctly different vantage points. Additional solutions within the high-dimensional solution design space may reveal alternate options to explore the variety of trajectory characteristics, or support a redesign to accommodate larger perturbations from the nominal deployment conditions.

CONCLUDING REMARKS

In this analysis, several low-thrust trajectories are constructed for a SmallSat, with each solution reaching a triangular equilibrium point from one of three rideshare opportunities. These two variables – the target equilibrium point and the deployment condition – are two significant drivers of the design space during mission concept development. Each of the trajectories presented in this analysis successfully terminates with bounded motion about the desired equilibrium point. These solutions tend to exhibit a variety of flight times between 2.57 years and 3.12 years. Further analysis of the impact of the thrust profile on the flight time for a fixed deployment condition and target equilibrium point is warranted and may potentially reveal further insight into the complexity of the solution space. Due to the construction of the initial guess for each trajectory, the required propellant mass for each solution presented in this analysis is approximately equal to 30.43 kg. Since this quantity is below the maximum available propellant mass, additional propellant may be used for post-insertion maneuvers or additional mass may be allocated to the payload. In addition to offering estimates of the flight time and required propellant mass – two important quantities during mission concept development – the results of this analysis also enable mission architecture trades. For instance, a spacecraft could reach either L4 or L5 from a single rideshare opportunity, validating the viability of low-cost, targeted science return using low-thrust-enabled SmallSats. The existence of trajectories to either L4 or L5 from the same deployment condition also indicates the potential for simultaneous deployment of two SmallSats. Each of these observations indicates the value of incorporating dynamical systems theory into rapid trajectory design strategies in support of SmallSat mission concept development.

ACKNOWLEDGEMENTS

Part of this research was carried out at the Jet Propulsion Laboratory, California Institute of Technology, under a contract with the National Aeronautics and Space Administration and funded through the Internal Strategic University Research Partnerships (SURP) program. Part of this research was also performed at the University of Colorado Boulder. Government sponsorship acknowledged.

REFERENCES

[1] M. Akioka, T. Nagatsuma, W. Miyake, K. Ohtaka, and K. Marubashi, "The L5 Mission for Space Weather Forecasting," *Advances in Space Research*, No. 1, 2005, pp. 65–69.

[2] N. Gopalswamy, J. Davila, O. St. Cyr, E. Sittler, F. Auchere, T. Duvall, J. Hoeksema, M. Maksimovic, R. MacDowall, A. Szabo, and M. Collier, "Earth-Affecting Solar Causes Observatory (EASCO): A potential International Living with a Star Mission from Sun-Earth L5," *Journal of Atmospheric and Solar-Terrestrial Physics*, 2011, pp. 658–663.

[3] M. L. Kaiser, T. A. Kucera, J. M. Davila, O. C. St. Cyr, M. Guhathakurta, and E. Christian, "The STEREO Mission: An Introduction," *Space Science Reviews*, No. 1-4, 2008, pp. 5–16.

[4] D. A. Ossing, T. A. Kucera, G. A. de Nolfo, and D. A. Quinn, "Journey 'Round the Sun: STEREO Science and Spacecraft Performance Results," *IEEE Aerospace Conference, Big Sky, MT*, 2018.

[5] A. Vourlidas, "Mission to the Sun-Earth L5 Lagrangian Point: An Optimal Platform for Space Weather Research," *Space Weather*, 2015, pp. 197–201.

[6] W. Schmidt and V. Bothmer, "Stereoscopic viewing of solar coronal and interplanetary activity," *Advances in Space Research*, No. 4/5, 1996, pp. 369–376.

[7] M. Lo, P. Llanos, and G. Hintz, "An L5 Mission To Observe The Sun and Space Weather, Part I," *20th AAS/AIAA Space Flight Mechanics Meeting, San Diego, CA*, 2010.

[8] P. Llanos, J. Miller, and G. Hintz, "Mission and Navigation Design of Integrated Trajectories to $L_{4,5}$ in the Sun-Earth System," *AIAA/AAS Astrodynamics Specialist Conference, Minneapolis, MN*, 2012.

[9] B. Lavraud, Y. Liu, K. Segura, J. He, G. Qin, M. Temmer, J. C. Vial, M. Xiong, J. Davies, A. Rouillard, R. Pinto, F. Auchre, R. A. Harrison, C. Eyles, W. G. P. Lamy, L. Xia, J. Eastwood, L. Kong, and J. G. Fernndez, "A small mission concept to the Sun-Earth Lagrangian L5 point for innovative solar, heliospheric and space weather science," *Journal of Atmospheric and Solar-Terrestrial Physics*, 2016, pp. 1–29.

[10] R. Sood and K. Howell, "L_4, L_5 Solar Sail Transfers and Trajectory Design: Solar Observations and Potential Earth Trojan Exploration," *26th AAS/AIAA Space Flight Mechanics Meeting, Napa, CA*, 2016.

[11] N. Bosanac, A. Cox, K. Howell, and D. C. Folta, "Trajectory Design for a Cislunar CubeSat Leveraging Dynamical Systems Techniques: The Lunar IceCube Mission," *Acta Astronautica*, 2018, pp. 283–296.

[12] N. Bosanac, F. Alibay, and J. R. Stuart, "A Low-Thrust Enabled SmallSat Heliophysics Mission to Sun-Earth L5," *IEEE Aerospace Conference, Big Sky, MT*, 2018.

[13] I. Elliott, C. J. Sullivan, N. Bosanac, F. Alibay, and J. R. Stuart, "Designing Low-Thrust-Enabled Trajectories for a Heliophysics SmallSat Mission to Sun-Earth L5," *29th AAS/AIAA Space Flight Mechanics Meeting, Ka'anapali, HI*, 2019.

[14] Busek Co. Inc., "BHT-200 Busek Hall Effect Thruster," Online; accessed December 2nd 2018.

[15] N. Bosanac, *Leveraging Natural Dynamical Structures to Explore Multi-Body Systems*. Ph.D. Dissertation, Purdue University, West Lafayette, IN, 2016.

[16] V. Szebehely, *Theory of Orbits: The Restricted Problem of Three Bodies*. London, UK: Academic Press, 1967.

[17] W. S. Koon, M. W. Lo, J. E. Marsden, and S. D. Ross, *Dynamical Systems, The Three-Body Problem and Space Mission Design*. Marsden Books, 2006.

[18] D. A. Vallado, *Fundamentals of Astrodynamics and Applications*. Microcosm Press, 4th ed., 2013.

[19] D. M. Goebel and I. Katz, *Fundamentals of Electric Propulsion: Ion and Hall Thrusters*. John Wiley Sons, 2008.

[20] T. A. Pavlak, *Trajectory Design and Orbit Maintenance Strategies in Multi-Body Dynamical Regimes*. Ph.D. Dissertation, Purdue University, West Lafayette, IN, 2013.

[21] W. Folkner, J. G. Williams, and D. H. Boggs, "The Planetary and Lunar Ephemeris DE421," *Interplanetary Network Progress Report, 42-178*, 2009.

[22] C. H. Acton, "Ancillary Data Services of NASA's Navigation and Ancillary Information Facility," *Planetary and Space Science*, No. 1, 1996, pp. 65–70.